

Layer-by-Layer Deposition: A Tool for Polymer Surface Modification

Wei Chen and Thomas J. McCarthy*

Polymer Science and Engineering Department, University of Massachusetts, Amherst, Massachusetts 01003

Received July 23, 1996; Revised Manuscript Received November 4, 1996

ABSTRACT: Layer-by-layer deposition of polyelectrolytes onto poly(ethylene terephthalate) (PET) film is reported as a method for polymer surface modification. Poly(allylamine hydrochloride) (PAH) and poly(sodium styrenesulfonate) (PSS) were sequentially adsorbed to unmodified (neutral) PET as well as PET samples that had been surface modified to contain carboxylate (PET-CO_2^-) and ammonium (PET-NH_3^+) functionality. XPS and contact angle data indicate that the layers are extremely thin (2–6 Å) and stratified to a significant extent. The wettability of the multilayer films is controlled by the outermost polyelectrolyte layer and the thickness of the individual layers (sublayers have an influence in multilayers with thinner layers). The substrate surface chemistry controls the thickness of all of the layers in the multilayer assembly as well as the stoichiometry (ammonium ion:sulfonate ion ratio) of the deposition process. The effect of the ionic strength of the polyelectrolyte solutions was studied for the case of the neutral substrate (PET); both the individual layer thickness and deposition stoichiometry are affected by ionic strength. Peel tests indicate that the multilayer assemblies have significant mechanical strength.

Introduction

Over the past several years, Decher and others^{1–12} have developed layer-by-layer deposition as a simple and versatile method for preparing supported multilayer thin films. These and other types of organic thin films show promise in applications such as sensors, friction-reducing coatings, integrated optics, and electronic device fabrication.¹³ The basic process involves dipping a charged (e.g. cationic) substrate into a dilute aqueous solution of an anionic polyelectrolyte and allowing the polymer to adsorb and reverse the charge of the substrate surface. The negatively charged coated substrate is rinsed and dipped into a solution of cationic polyelectrolyte, which adsorbs and re-creates a positively charged surface. Sequential adsorptions of anionic and cationic polyelectrolytes allow the construction of multilayer films.

The process has several important advantages over other techniques for preparing ordered multilayer thin films: the assembly is based on spontaneous adsorptions, the substrate can have, in principle, any size, shape, topography, or topology, and no stoichiometric control is necessary to maintain surface functionality—defects do not propagate. This simple, but powerful preparative technique is clearly in its infancy. The synthesis of polyelectrolytes for layer-by-layer deposition (with controlled charge density, charge location, and functionality), adsorptions from nonaqueous solutions, competitive adsorptions to prepare mixed layers, and chemical reaction of adsorbed layers are obvious directions that will expand the utility of this versatile technique.

We have been involved in a program directed at controlling solid polymer surface properties through chemical manipulation of surface functionality.^{14–21} Our approach is to introduce a discrete functional group (e.g. alcohol, $-\text{OH}$) by chemical reaction(s) at solid–solution interfaces. The surface can be further derivatized to a series of chemically different surfaces through well-controlled chemical reactions of this functional group.

This type of modification has the advantage that chemically well-defined surfaces are prepared which are amenable to fundamental surface structure–surface property correlations. The clear disadvantage of this approach is that it is rarely practical. The practical approaches to polymer surface modification include flame treatment, corona discharge treatment, plasma modification, and surface graft polymerization.²² These have the disadvantage that chemically well-defined surfaces cannot be designed and prepared, but the advantage that they work to control the technologically significant properties of adhesion, wettability, biocompatibility, and gas permeability. Multistep chemical reactions will certainly not replace the more simple and practical approaches for most applications—even if they are more well understood.

Layer-by-layer deposition may offer the advantages of both these approaches as a surface modification technique for polymers. It is a simple, relatively fast, environmentally benign, and potentially economical process. Surface functionality can be controlled directly by choosing appropriate polyelectrolytes.

We report here the surface modification of poly(ethylene terephthalate) (PET) using layer-by-layer deposition. PET is an economically important thermoplastic that is used as photographic film, magnetic recording tape, packaging material, and electronic insulation.²³ PET has been surface modified by a variety of techniques including plasma,²⁴ corona discharge,²⁵ ion beam,²⁶ laser treatment,²⁷ photoinitiated graft polymerization,²⁸ saponification,²⁹ aminolysis,^{30,31} reduction,^{31,32} and entrapment of poly(ethylene oxide).³³ PET was chosen as the substrate for modification studies for several reasons: (1) It contains carbonyl groups that are capable of hydrogen bonding. (2) The surface can be readily hydrolyzed to introduce carboxylic acid (as well as alcohol) functionality that can support negative charge (PET-CO_2^-) in sufficiently basic solution. (3) The surface can react with polyamines to incorporate amine functionality that can support positive charge (PET-NH_3^+) in nonbasic solution.

We chose poly(sodium styrenesulfonate) and poly(allylamine hydrochloride) as polyelectrolytes for surface modification because this system has been most widely

* Abstract published in *Advance ACS Abstracts*, December 15, 1996.

studied and documented. The techniques of contact angle analysis and X-ray photoelectron spectroscopy were used for analysis and proved effective in indicating the structure of the outermost layers, the individual layer thicknesses, and the overall multilayer thicknesses.

Experimental Section

General Procedures. Poly(allylamine hydrochloride) ($M_w = 50\,000$ – $65\,000$) and poly(sodium styrenesulfonate) ($M_w = 70\,000$) were obtained from Aldrich. Sodium chloride, $MnCl_2 \cdot 4H_2O$, 1 M HCl, sodium hydroxide, methanol (HPLC grade), and hexane (HPLC grade) were purchased from Fisher. All materials were used as received. Water was purified using a Millipore Milli-Q system that involves reverse osmosis followed by ion-exchange and filtration steps. Buffer solutions used for contact angle measurement were CRC standard.³⁴ Solution pH for layer-by-layer adsorption studies was adjusted with either HCl or NaOH solution using a Fisher 825MP pH meter. X-ray photoelectron spectra (XPS) were recorded on a Perkin-Elmer-Physical Electronics 5100 spectrometer with Al K α excitation (15 kV, 400 W). Spectra were taken and recorded at two different take-off angles, 15° and 75° between the plane of the sample surface and the entrance lens of the detector optics. Atomic concentration data were determined using sensitivity factors obtained from samples of known composition: C_{1s}, 0.201; O_{1s}, 0.540; N_{1s}, 0.385; S_{2p}, 0.440. Contact angle measurements were made with a Ramé-Hart telescopic goniometer and a Gilmont syringe with a 24-gauge flat-tipped needle. Probe fluids were either water (purified as described above) or buffer solutions. Dynamic advancing (θ_A) and receding angles (θ_R) were recorded while the probe fluid was added to and withdrawn from the drop, respectively. Peel tests were performed manually with an angle of 180° between the delaminated film surface and tape (3M no. 810).

Substrate Preparation. PET films (Mylar, 5 mil) were rinsed with distilled water and methanol, extracted in refluxing hexane for 2 h, and then dried (room temperature, 0.01 mm, >24 h). PET-CO₂⁻ was prepared by introducing clean PET to 1 M NaOH aqueous solution for 16 min at 60 °C. The film was subsequently rinsed with 0.1 M HCl, distilled water (2×), methanol, and then hexane, and dried at reduced pressure. PET-NH₃⁺ was prepared by immersing clean PET film in PAH solution (167 mg of PAH in 120 mL of water, pH = 11.5) for 1 h at room temperature. The film was removed from the solution, rinsed with water three times, and introduced to water adjusted to pH = 2.2 for 30 min. After rinsing with three aliquots of water, the PET-NH₃⁺ film samples were dried at reduced pressure.

Layer-by-Layer Deposition. Adsorptions were carried out at room temperature in open beakers containing unstirred polyelectrolyte solutions that were prepared fresh every day. After every layer deposition, film samples were rinsed with water (purified as described above) three times. After the desired number of layers had been deposited, films were dried at reduced pressure before characterization.

Results and Discussion

Substrate Preparation. Commercial poly(ethylene terephthalate) film (5 mil DuPont Mylar) was used to prepare three substrates for layer-by-layer deposition. The film was rinsed with water and then methanol, extracted with hexane, and dried to constant mass to prepare "unmodified polyester" (PET).

PET was hydrolyzed using 1 M aqueous NaOH for 16 min at 60 °C and subsequently protonated to prepare PET-CO₂H. This surface contains a mixture of carboxylic acid and alcohol functional groups and is negatively charged at sufficiently high pH. The conditions for hydrolysis were chosen to maximize surface carboxylic acid concentration and minimize polymer degradation (hydrolysis results in chain scission). Kinetics of the hydrolysis of PET at 60 °C were monitored by water

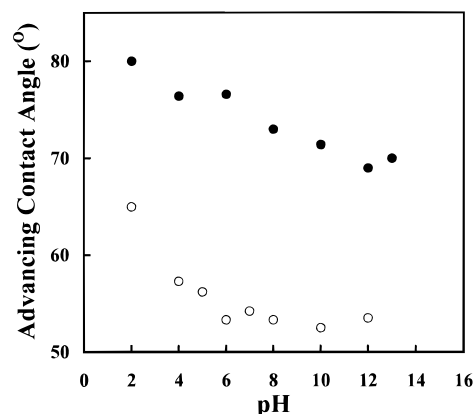


Figure 1. Contact angles (θ_A) of buffered aqueous solutions on PET (●) and PET-CO₂H/PET-CO₂⁻ (○) film.

contact angles, XPS, and gravimetric analysis. After reaction for 16 min, the contact angles reached a minimum value ($\theta_A/\theta_R = 62^\circ/16^\circ$), oxygen content as determined by XPS (15° take-off angle) was maximized (O, 30.1%; C, 69.9%), and no degradation (mass loss) was observed. PET exhibits contact angles of $\theta_A/\theta_R = 77^\circ/55^\circ$ and XPS atomic concentrations of O, 28.5%; C, 71.5%. Longer hydrolysis times did not lead to lower contact angles or increased oxygen content. That PET-CO₂H is capable of supporting negative charge is indicated by the dependence of contact angle on the pH of the probe fluid. Figure 1 shows the advancing contact angles of buffered aqueous solutions on PET-CO₂H as well as on unmodified PET. The lower contact angles at higher pH values indicate the presence of -CO₂H that ionizes to -CO₂⁻ groups. The advancing contact angle data for PET are not completely independent of the pH of the probe fluid. Contact angles of higher pH solutions are slightly lower as hydrolysis of PET occurs during contact angle analysis. This is observed clearly in the receding contact angle data. PET exhibits $\theta_R = 55^\circ$ with water, $\theta_R = 42^\circ$ with pH = 10 buffer, and $\theta_R = 22^\circ$ with pH = 12 buffer. Receding contact angles of fluids that are reactive toward the substrate depend on the conditions (rate) of determining these dynamic values.

A PET substrate capable of supporting a positive charge (PET-NH₃⁺) was prepared by allowing poly(allylamine hydrochloride) (PAH) to adsorb to/react with PET at elevated pH (as the free base). PAH adsorbs to PET at low pH (see below) but reacts by amidation at high pH as the free base to form a covalently attached PAH layer. The adsorption/reaction of PAH with PET was studied over the pH range 1.87–11.84. Figure 2 shows XPS atomic composition data (nitrogen, 15° take-off angle) for PET samples treated with aqueous PAH (0.02 M repeat units) at room temperature for 1 h as a function of solution pH. A sharp increase in nitrogen content occurs at pH = ~10. The pK_a of PAH is ~10.6;^{35,36} thus the sharp increase can be attributed to the loss of charge-charge repulsions in deprotonated PAH. XPS analysis indicates that amidation is extensive. Atomic composition of the sample prepared at pH = 11.84 was C, 82.3%; O, 10.63%; N, 6.7%; amidation is indicated by the low oxygen content (loss of high oxygen content ethylene glycol). A physisorbed layer of PAH (C:N = 3) on PET (C:O = 2.5) with this nitrogen content would have an atomic composition of C, 72.4%; O, 20.9%; N, 6.7%. Amidation is also indicated from the binding energy of the N_{1s} photoelectron line in samples prepared at high pH. PAH adsorbed from low-

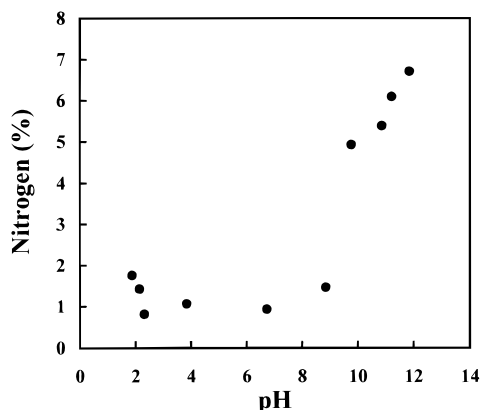
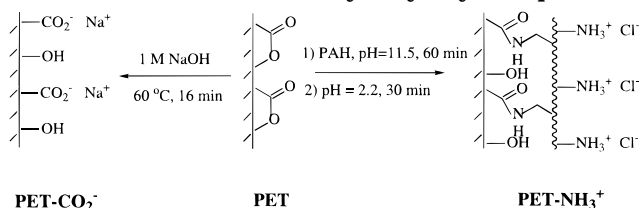


Figure 2. XPS atomic concentration (nitrogen) for PET film samples treated with aqueous PAH as a function of pH.

Scheme 1. Substrates for Layer-by-Layer Deposition



pH solutions exhibits a peak with a N_{1s} binding energy of ~ 403 eV. The corresponding photoelectron line for PAH adsorbed at high pH is ~ 400 eV. The 3 eV difference in binding energy is due to the fact that N_{1s} electrons in $-\text{NH}_3^+$ are more strongly bound than in $-\text{NH}_2/\text{CONH}-$. Protonation (exposure to $\text{pH} = 2.2$ solution) produced a broad N_{1s} line spanning the 400–403 eV range, indicating the presence of both amide and $-\text{NH}_3^+$.

PET- NH_2 samples prepared at high pH contain physisorbed poly(allylamine) as well as chemisorbed (covalently attached through amide linkages) poly(allylamine). Kinetics of the adsorption/reaction (amidation) at $\text{pH} = 11.5$ were studied to 7 h; the nitrogen content reached a plateau value of $\sim 6.5\%$ (15° take-off angle) after 30 min. Samples prepared at $\text{pH} = 11.5$ for 60 min were soaked in $\text{pH} = 2.2$ solution and desorption kinetics were determined to 100 min. The nitrogen content decreased to a minimum value $\sim 5\%$ after 10 min. PET- NH_3^+ samples used for further experiments were prepared by adsorption of/reaction with poly(allylamine) (0.02 M repeat units) for 60 min at $\text{pH} = 11.5$ followed by desorption for 30 min at $\text{pH} = 2.2$. Scheme 1 summarizes the routes to the charged substrates used for layer-by-layer adsorption. In an attempt to determine relative charge densities of the PET- NH_3^+ and PET- CO_2^- substrates, we reacted PET- CO_2H with 1,1'-carbonyldiimidazole, a reagent that converts carboxylic acids to acyl imidazolides. XPS indicates that there is $\sim 0.7\%$ nitrogen on the reacted surface (there are two nitrogen atoms per carboxylic acid group). This corresponds to about one carboxylic acid functional group per twenty PET repeat units. There is $\sim 5\%$ nitrogen on the PET- NH_3^+ surface and about half of that is present as PET- NH_3^+ (the nitrogen peak at ~ 403 eV) and the other half is due to $-\text{CONH}-$ (the peak at ~ 400 eV). The charge density on the PET- NH_3^+ surface is thus significantly greater (~ 7 -fold) than on PET- CO_2^- (assuming that the reaction with 1,1'-carbonyldiimidazole is quantitative).

Initial Polyelectrolyte Adsorptions. Conditions for layer-by-layer deposition of poly(allylamine hydro-

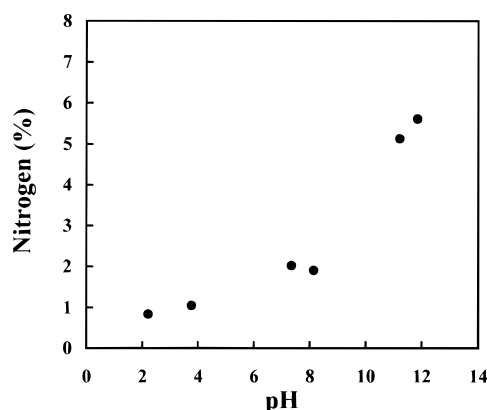


Figure 3. XPS atomic concentration (nitrogen) for PET- CO_2^- film samples with one PAH layer adsorbed as a function of pH of the adsorption solution.

chloride) (PAH) and poly(sodium styrenesulfonate) (PSS) were modeled after those reported by Decher^{1,2} for inorganic substrates modified by silanation to contain ammonium ions. PAH was used as the polyelectrolyte for the first layer adsorption³⁷ to PET and PET- CO_2^- ; PSS was used as the initial polyelectrolyte for PET- NH_3^+ . For consistency, this PSS layer is referred to in this paper as the second layer and the covalently attached PAH is regarded as the first layer. Thus all samples described that contain an even number of layers have PSS as the outermost layer and samples with an odd number of layers contain PAH as the outermost layer.

A series of initial experiments were carried out to compare polyelectrolyte adsorption behavior onto the organic substrates with the reported results^{1,2} for inorganic substrates. Adsorption kinetics, polyelectrolyte concentration effects, and the effect of ionic strength of the solution were studied. The effect of solution ionic strength is discussed below and is similar to that observed for inorganic substrates. PAH concentration was varied from 0.006 to 0.024 M (repeat units) and PSS concentration was varied (for the second layer adsorption to PET) from 0.008 to 0.025 M (repeat units). There was no variation in adsorbed amount as determined by XPS over these concentration ranges. Kinetics indicates that adsorption is rapid when driven by electrostatic interaction (substrate and polyelectrolyte are charged oppositely), reaching a final adsorbed amount (we consciously do not use the term equilibrium³⁸) in less than 10 min. The adsorption is noticeably slower when the surface is uncharged (PET). The adsorbed amount of PAH (0.02 M repeat units in 0.01 M HCl, $\text{pH} = 2.2$) on PET increased with adsorption time up to 30 min as assessed by XPS. The nitrogen content of the PET-PAH surface did not increase further after 370 min total adsorption time. An adsorption time of 60 min for deposition of the first PAH layer on PET was used in all subsequent experiments. The kinetics of adsorption of the second layer (PSS) onto PET-PAH indicates that a rapid adsorption occurs, complete in less than 10 min. Adsorption times of 20 min were used for all experiments described except for adsorption of the first PAH layer onto neutral PET.

The adsorption of PAH onto PET- CO_2^- (PET- CO_2H at low pH) warrants mention because of its dependence on pH. Figure 3 shows XPS nitrogen atomic concentration data as a function of the pH of the PAH solution (0.02 M repeat units, 60 min adsorption time). Three distinct regions are evident. At low pH the nitrogen

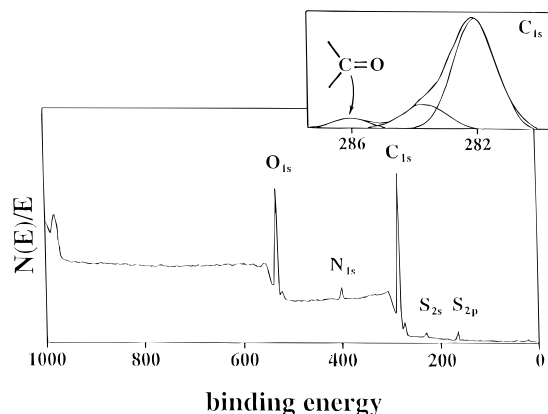


Figure 4. Survey and C_{1s} region XPS spectra of a four-layer polyelectrolyte film supported on $PET-CO_2^-$.

content is low; the charged polymer (PAH) adsorbs to the neutral $PET-CO_2H$ surface with low coverage. The interaction between the polyelectrolyte and the surface is weak (likely hydrogen bonding between ammonium protons and acid carbonyl groups³⁹) and charge-charge repulsions between ammonium ions force the chain to spread out on the surface, leading to a submonolayer coverage. At pH = 6–8 the nitrogen content is significantly higher. In this pH range, both the polyelectrolyte and $PET-CO_2^-$ surface (see Figure 1) are charged and the electrostatic attraction leads to more dense coverage. At high pH PAH is neutral and adsorbs to the charged $PET-CO_2^-$ surface as a more collapsed coil than when protonated, giving rise to high nitrogen content. Amidation (see above) may occur under these conditions as it does with PET. Adsorptions of polyelectrolytes on $PET-CO_2^-$ in the experiments described below were carried out at pH = 8, conditions under which both the polyelectrolyte and the surface are charged.

Multilayer Assembly. Except for the conditions noted above, PAH/PSS multilayers were built up on PET, $PET-CO_2^-$, and $PET-NH_3^+$ using conditions essentially identical to those reported for inorganic substrates. The effect of polyelectrolyte solution ionic strength was studied for PET. Substrates were dipped in 0.02 M polyelectrolyte solution (pH = 2.2, except for $PET-CO_2^-$, in which case pH = 8), removed after 20 min, rinsed with three aliquots of water, and then dipped in the oppositely charged polyelectrolyte solution. After the desired number of layers were deposited, the polymer film-supported multilayers were rinsed a final three times with water and were dried at room temperature at reduced pressure before XPS and contact angle analyses.

Much of the details that follow concern variable take-off angle XPS analysis of the multilayer films and the PET substrate immediately beneath the multilayer assembly. Survey and C_{1s} region spectra of a four-layer film supported on $PET-CO_2^-$ ($PET-CO_2^-$ -PAH-PSS-PAH-PSS) are shown in Figure 4. Most of the features of interest are present in these spectra. The intensities of the N_{1s} (403 eV) and S_{2p} (167 eV) photoelectron lines can be used to assess the relative concentrations of PAH and PSS and degree of stratification (layer segregation) in the multilayers. The carbonyl C_{1s} photoelectron line is due entirely to the PET substrate; this peak decreases in intensity and eventually disappears as more layers are deposited. We can estimate (we could calculate if the mean free path were known) the thickness of the multilayer assemblies and individual layers from the decrease in intensity of this substrate peak.

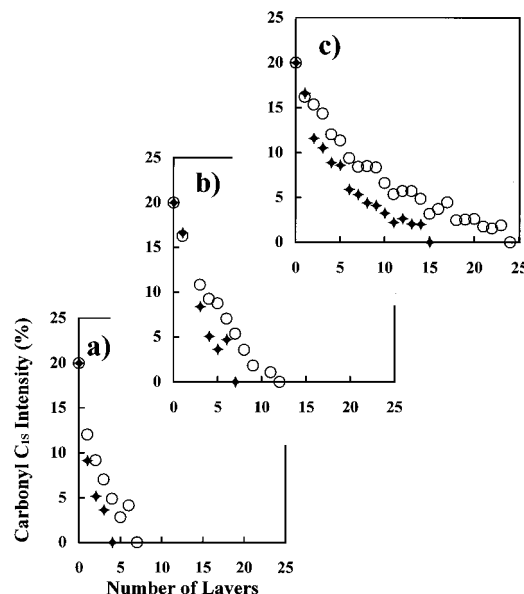


Figure 5. Carbonyl C_{1s} intensity (expressed as the percentage of total carbon intensity) versus the number of layers in the multilayer assembly: (a) $MnCl_2$ present in both PAH and PSS solutions; (b) $MnCl_2$ present in only the PSS solution; (c) no $MnCl_2$ in polyelectrolyte solutions. The closed (\blacklozenge) and open (\circ) symbols are data recorded at 15° and 75° take-off angles, respectively.

Multilayer Deposition on PET. Three series of experiments were carried out to surface modify the neutral PET substrate using layer-by-layer deposition. In these experiments manganese chloride (1.0 M $MnCl_2$) was added to either both PAH and PSS solutions, only the PSS solution, or neither polyelectrolyte solution. The addition of salt has been demonstrated^{1,2} to increase the thickness of the layers by screening charge-charge repulsions during adsorption. Figure 5 shows XPS data indicating that this effect is also observed with the PET substrate. Plotted is the atomic concentration of carbonyl carbons (as percentage of total carbon detected) versus the number of layers in the supported multilayer. The carbonyl C_{1s} photoelectrons (Figure 4) originate only in the substrate, and this signal is attenuated as polyelectrolyte layers are applied. The data clearly indicate the effect of $MnCl_2$ on thickness. At 15° take-off angle the carbonyl C_{1s} peak is completely attenuated after application of 4 layers when $MnCl_2$ is present in both solutions, 7 layers when $MnCl_2$ is present in the PSS solution, and ~ 15 layers when no $MnCl_2$ is present. The 75° data exhibit the same trend. The scatter in the data is due in large part to the fact that separate samples were used for analysis of each thickness (number of layers) multilayer. Samples were not used after analysis as substrates for further depositions.

The C_{1s} peak intensity should decrease exponentially with the buildup of the multilayers, and the data (Figure 5) qualitatively fit the predicted decay, but the take-off angle dependence is confusing. Equation 1⁴⁰ expresses the attenuation of photoelectron intensity in solids as a function of sampling depth, where N_0 is the

$$N = N_0 e^{-t/\lambda \sin \theta} \quad (1)$$

number of photoelectrons that originate at depth t , N is the number of photoelectrons emitted from the solid that have not been inelastically scattered, λ is the mean free path of the electron, and θ is the take-off angle. This expression indicates that 95% of detected photo-

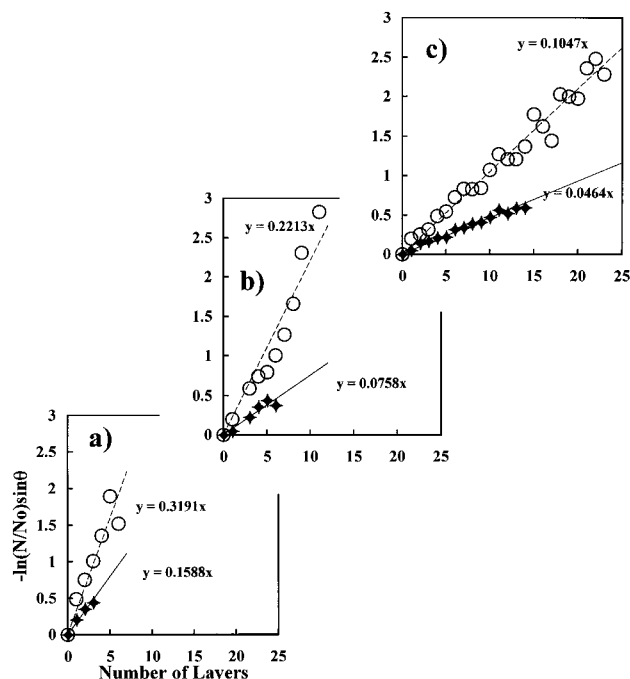


Figure 6. Plots of $-\ln(N/N_0) \sin \theta$ vs number of layers in the multilayer film. The slopes of the lines indicate the ratio of the average layer thickness to the C_{1s} photoelectron mean free path: (a) $MnCl_2$ present in both PAH and PSS solutions; (b) $MnCl_2$ present in only the PSS solution; (c) no $MnCl_2$ in polyelectrolyte solutions. The closed (\bullet) and open (\circ) symbols are data recorded at 15° and 75° take-off angles, respectively.

electrons originate in the outermost $3\lambda \sin \theta$; thus the carbonyl C_{1s} peak should be attenuated to 5% of its original intensity when the multilayer film thickness is $3\lambda \sin \theta$. Equation 1 also indicates that the spectra recorded at a take-off angle of 15° assess the composition of the outermost $\sim 27\%$ of the region analyzed at 75° take-off angle. These principles predict that the carbonyl C_{1s} peak intensity should decrease exponentially from 20% (2 of 10 carbons in the PET repeat unit are carbonyls) to 1% when the multilayer thickness reaches $3\lambda \sin \theta$ (0.78 λ for 15° and 2.90 λ for 75°) and that it should take ~ 4 times as many layers to attenuate the 75° carbonyl signal to the same extent that the 15° signal is attenuated.

The data in Figure 5 do not support the latter prediction; in all three cases fewer than twice as many layers are required to attenuate the 75° signal to the same extent that the 15° signal is attenuated. Our explanation for this inconsistency is that the mean free paths of electrons in these layered materials have an angular dependence: Rearranging eq 1 and substituting nz for t , where n is the number of layers and z is the average thickness of the individual layers, yield the expression in eq 2. In Figure 6 are plots of $-\ln(N/N_0) \sin \theta = nz/\lambda$

$$-\ln(N/N_0) \sin \theta = nz/\lambda \quad (2)$$

$\sin \theta$ versus n , where N is the atomic concentration of carbonyl carbons (data from Figure 5) and N_0 is the carbonyl carbon concentration for virgin PET. The overall linearity of the data shows that individual layer thicknesses are close to constant and the slopes of the lines indicate the average layer thickness divided by the photoelectron mean free path. In each case, longer mean free paths (approximately twice as long) are indicated by the lower slopes of the 15° take-off angle data. Apparently, the structure of these multilayer

assemblies allows the "channeling" of electrons at angles close to the plane of layer buildup. The stratification of these structures is discussed below. An alternative explanation for the small take-off angle dependence is surface roughness. We discount this possibility because we have prepared modified PET surfaces using the same film that show pronounced take-off angle-dependent spectra. We have carried out limited scanning electron microscopy studies on layer-by-layer assemblies on PET- NH_3^+ and PET- CO_2^- surfaces. In each case, the surfaces become smoother after 20 layers have been deposited.

We can estimate the thickness of the layers and multilayers using estimates of the electron mean free path. Values for λ in organic polymers are somewhat controversial, ranging from the low values reported by Clark^{41,42} to higher values reported by others.^{43,44} Ashley and co-workers have developed a theoretical approach to the problem⁴⁵⁻⁴⁸ and calculate mean free paths based on bulk density and molecular structure. The mean free paths of electrons in layer-by-layer assemblies have not been discussed in the literature and as discussed above are certainly a function of the supermolecular structure of the multilayers. We have calculated⁴⁹ a mean free path for Si_{2p} electrons in PAH/PSS multilayers using both XPS and X-ray reflectivity analysis of films built up on aminobutyldimethylmethoxysilane-treated silicon wafers. A film consisting of 8 layers (4 PAH/PSS bilayers) attenuates $>95\%$ of the Mg $K\alpha$ -excited Si_{2p} photoelectron intensity at 75° take-off angle (is $\sim 3\lambda$ thick) and is 61 Å thick (including the silane coupling agent) as assessed by X-ray reflectivity. A mean free path of ~ 20 Å for the Si_{2p} electron is indicated. The XPS data reported in this paper were acquired using Al $K\alpha$ excitation; we calculate⁵⁰ a mean free path of ~ 19 Å for the C_{1s} photoelectron. The slopes of the 75° data in Figure 6 yield average layer thicknesses of 6.1, 4.2, and 2.0 Å for multilayers prepared with $MnCl_2$ added to both PAH and PSS solutions, only the PSS solution, and neither polyelectrolyte solution, respectively. These values must be regarded only as estimates as we make the assumption that the mean free paths at 75° take-off angle in the PET-supported multilayers are the same as the value determined for the silicon-supported multilayer film. Nevertheless, the data indicate extremely thin individual layers, much thinner in the case of no added $MnCl_2$, than the layers that form on inorganic substrates. We emphasize that these are average thickness values determined from the slopes of the lines in Figure 6 (dividing the total multilayer assembly thickness by the number of layers) and that the individual layers, while uniform, are not dense, close-packed monolayers, but are interdigitated at functional group dimensions. That the layers are quite rigorously stratified is discussed below. We believe that the multilayer assemblies are quite dense; gas permeability measurements¹⁰ on a very similar system (PAH/PSS multilayers supported on surface-oxidized poly(4-methyl-1-pentene)) indicate that the multilayers exhibit good gas barrier properties.

XPS atomic composition data for nitrogen and sulfur are uniformly consistent with the carbonyl intensity data discussed above. Figure 7 shows plots of sulfur and nitrogen atomic concentration as a function of the number of layers in the multilayer film for the series of samples prepared with no added $MnCl_2$. The atomic composition levels after a sufficient number of layers (~ 15 at 15° and ~ 18 at 75° take-off angle) have been

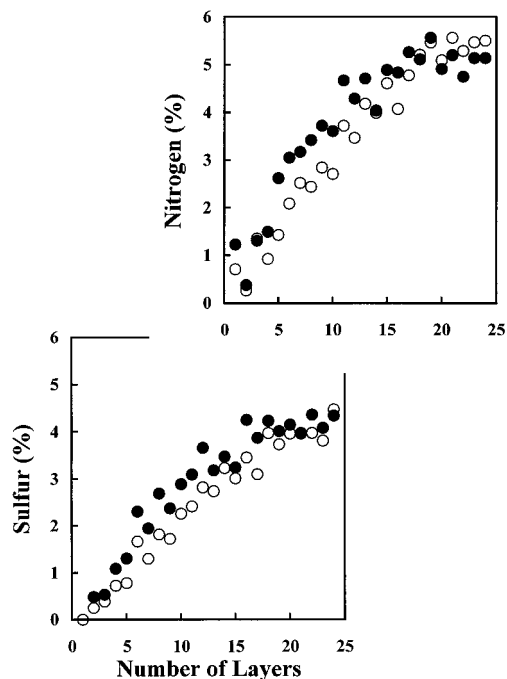


Figure 7. Sulfur and nitrogen atomic concentrations determined at 15° (●) and 75° (○) take-off angles as a function of the number of layers in the multilayer film. The multilayers were built up on PET using polyelectrolyte solutions containing no added salt.

deposited to completely attenuate the C_{1s} and O_{1s} photoelectrons of PET. The unexpectedly small dependence on take-off angle is apparent, again indicating an angular-dependent electron mean free path. The sulfur and nitrogen atomic composition (data not shown) for the series of samples prepared with $MnCl_2$ in both solutions level after ~5 layers (15°) and 7 layers (75°) have been adsorbed. Corresponding data for the samples prepared with $MnCl_2$ in only the PSS solution (also not shown) level at ~8 (15°) and 12 (75°) layers.

Sulfur:nitrogen atomic ratio data for the three series of polyelectrolyte multilayers are shown in Figure 8. The ratios shown were obtained using 75° take-off angle data; 15° data yield nearly identical ratios due to the near absent take-off angle dependence and the fact that the substrate contains no nitrogen or sulfur. These ratioed data are shown to make three points concerning the structures of the multilayers. First, there is a pronounced odd–even trend in all three sets of data that persists to high layer number, where the addition of one more PSS or PAH layer does not greatly affect the composition of the multilayer assembly. The S:N ratio is relatively high when the outermost layer is PSS and relatively low when the top layer is PAH. This suggests that the layers, even though they are not close-packed monolayers, are stratified. Second, the amplitude of the odd–even trend increases with increasing layer thickness; the exponential decay of photoelectron intensity with depth (eq 1) results in an effective enhancement of the signal from the outermost layer and this enhancement is greater with increasing layer thickness. Third, the stoichiometry of the assembly process (ammonium ion:sulfonate ion ratios) is evident from those data and we note that it is different for each of the series studied. With no $MnCl_2$ in the polyelectrolyte solutions the S:N ratio is ~0.75, indicating that there are approximately 4 ammonium ions per 3 sulfonate ions in the multilayer assembly. With $MnCl_2$ present only in the PSS solution, the ratio is close to unity. With $MnCl_2$ present in both

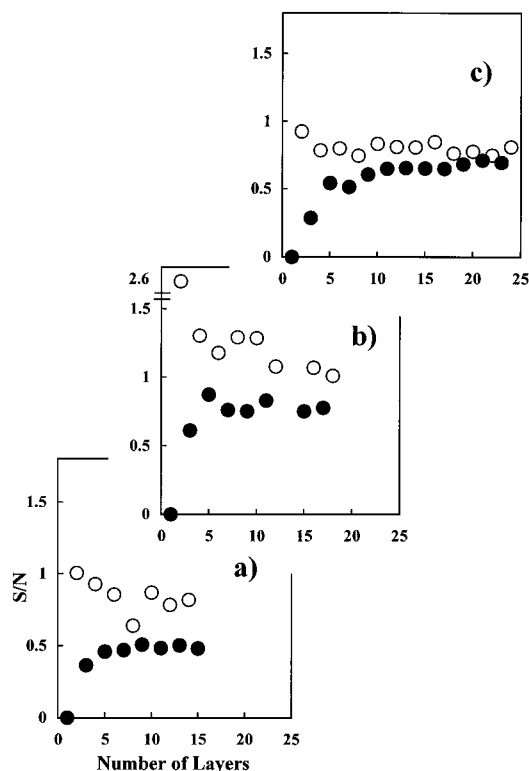


Figure 8. Sulfur:nitrogen atomic ratio data (75° take-off angle data) for the three series of polyelectrolyte multilayers: (a) $MnCl_2$ present in both PAH and PSS solutions; (b) $MnCl_2$ present in only the PSS solution; (c) no $MnCl_2$ in polyelectrolyte solutions (odd number of layers (●); even number of layers (○)).

solutions, the S:N ratio is ~0.65, which indicates a ~3:2 ratio of ammonium to sulfonate ions. These data emphasize two interesting features of layer-by-layer deposition: the self-assembly process exerts its own stoichiometric control and a particular stoichiometry is not required.

Water contact angle data also indicate the stratified structure of the multilayer assemblies with odd–even trends.⁵¹ Figure 9 shows advancing contact angle data for each of the three series of samples. Contact angle is in general a more surface-selective technique than XPS, and the contact angle data level after fewer layers are applied (compare with Figures 5 and 7). The contact angles for samples with an odd number of layers (PAH as the outermost layer) are different for each of the series of samples: when $MnCl_2$ was used in both polyelectrolyte solutions, $\theta_A = 70 \pm 1^\circ$ (for 3-, 5-, 7-, 9-, and 11-layer films); for samples prepared with $MnCl_2$ in only the PSS solution, $\theta_A = 60 \pm 1^\circ$ (for 5-, 7-, 15-, and 17-layer films); and for samples prepared without $MnCl_2$, $\theta_A = 46 \pm 1^\circ$ (for 9-, 11-, 13-, 15-, and 19-layer films). The increase in wettability with decreasing layer thickness is due to an increasing contribution to the contact angle from the underlying PSS layer, which is more wettable than PAH. There is less of a layer thickness effect for the samples containing an even number of layers (PSS as the outermost layer). For both series using $MnCl_2$ in the PSS solution, the contact angle levels at $\theta_A = 45 \pm 2^\circ$ and for the series without $MnCl_2$, at $\theta_A = 53 \pm 1^\circ$. The outermost PSS layer more effectively (than PAH) screens the underlying layer from the contact angle analysis. The receding contact angle data (not shown) are less lucid as the values for both odd and even number-of-layer samples are very similar. The series prepared with $MnCl_2$ in both polyelectrolyte solutions did exhibit a statistically significant odd–even

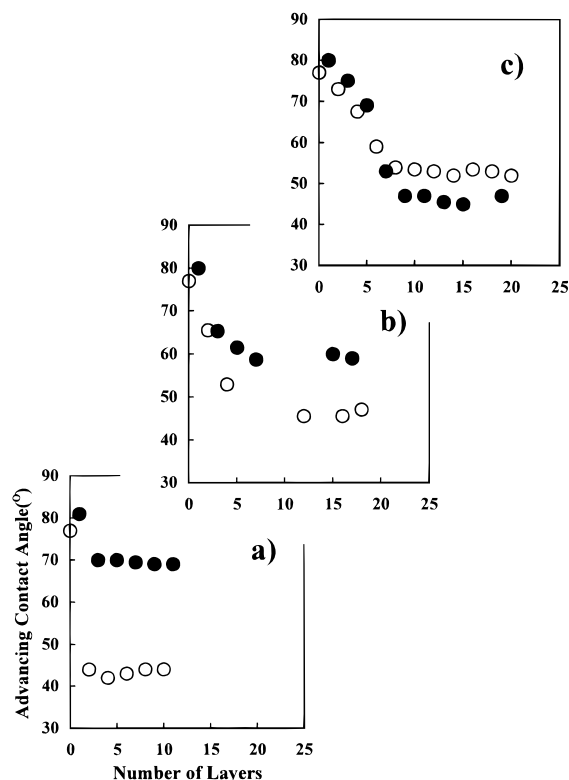


Figure 9. Advancing contact angle data for each of the three series of samples: (a) MnCl_2 present in both PAH and PSS solutions; (b) MnCl_2 present in only the PSS solution; (c) no MnCl_2 in polyelectrolyte solutions (odd number of layers (●); even number of layers (○)).

trend (the other two series did not), with θ_R oscillating between $22 \pm 2^\circ$ and $16 \pm 1^\circ$.

We made attempts to follow the layer-by-layer assembly stoichiometry using XPS data for the counterion (manganese, sodium, and chloride) concentrations. For the cases in which no MnCl_2 was added to the polyelectrolyte solutions and in which MnCl_2 was added to only the PSS solution, the atomic concentrations of sodium, chlorine, and manganese were on the order of instrument noise and meaningful data were not obtained. For the case with MnCl_2 in both solutions, the manganese and chlorine concentrations were high enough to measure (no sodium was observed), but we caution the use of these data for quantitative analysis for two reasons: the values are at the sensitivity limits of XPS and because the counterions are most certainly not distributed homogeneously throughout the multilayer assembly, a quantitative analysis would be biased. Figure 10 shows manganese and chlorine atomic concentration data as a function of the number of layers deposited. The chlorine concentration oscillates from high in odd number-of-layer samples (PAH as outermost layer) to low in even number-of-layer samples (PSS as outermost layer). The manganese concentration oscillates with the reverse trend up to 10 layers: high when PSS is the outermost layer and zero when PAH is the outermost layer.⁵² These general trends are expected, but after 10 layers have been deposited, no chlorine is observed in even number-of-layer samples and no manganese is observed at all. As the N:S ratio is greater than 1 for all samples (Figure 8), chloride should be present as the counterion for the excess ammonium ion in all samples—we cannot readily explain its absence. The absence of manganese in the 12- and 14-layer samples is readily explained by the excess of ammonium ions

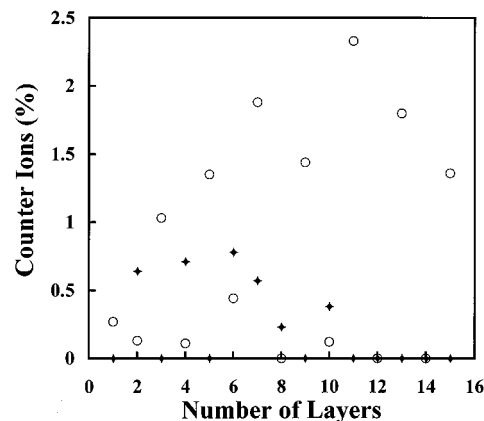


Figure 10. Manganese (◆) and chlorine (○) atomic concentrations from 75° take-off angle XPS data as a function of number of layers in the multilayer film prepared with MnCl_2 in both PAH and PSS solutions.

present, but these multilayer assemblies apparently contain no free (from ammonium ion) sulfonate groups (the surfaces must not be negatively charged) to induce the adsorption of the next PAH layer; however, the PAH layers clearly adsorb (Figure 8). We conclude that these discrepancies must be due to the analytical technique: the counterion contents of the multilayer assemblies observed by XPS (at high vacuum) must not accurately reflect the structure of the assemblies when in contact with aqueous media.

Multilayer Deposition on PET-CO_2^- and PET-NH_3^+ . Multilayer assemblies were built up on the charged substrates in the same manner described for PET except that for PET-CO_2^- , the polyelectrolyte solutions were adjusted to pH = 8 and for PET-NH_3^+ , PSS was adsorbed first. The effect of adding MnCl_2 to the adsorption solutions was not examined. In general, the layer-by-layer assembly processes proceed in the same manner as for PET and the structures of the multilayer films produced are similar; we have characterized these samples to the same extent as those supported on PET, but we present only limited data here. Figure 11 shows sulfur:nitrogen atomic ratio data (75° take-off angle) for multilayers built up on these substrates as a function of the number of layers adsorbed. The odd–even trend indicating layer stratification is evident as was the case for neutral PET (Figure 8). The advancing water contact angle data (not shown) also show an odd–even trend with $\theta_A = \sim 61^\circ$ (odd, PAH outermost layer) and $\theta_A = \sim 53^\circ$ (even, PSS outermost layer) for PET-CO_2^- -supported multilayer films and $\theta_A = \sim 60^\circ$ (odd) and $\theta_A = \sim 50^\circ$ (even) for PET-NH_3^+ substrates.

The presence of surface charge does affect the individual layer thicknesses. Figure 12 shows plots of the type discussed above (Figure 6) for determining average layer thickness based on carbonyl C_{1s} photoelectron attenuation. The PET-CO_2^- -supported layers are 2.1 times as thick as the PET-supported layers (no added MnCl_2). Using the 75° take-off angle data, a C_{1s} electron mean free path of 19 Å, and the assumptions discussed above, the average layer thickness is calculated to be 4.1 Å. The PET-NH_3^+ -supported layers are 1.4 times as thick (2.8 Å) as those on PET. The initial surface charge “screens” charge–charge repulsions in the adsorbing polyelectrolyte, allowing a greater adsorbance and thicker resulting layers. The stoichiometry of the assembly process (ammonium ion:sulfonate ion ratios) is also affected by the substrate surface chemistry

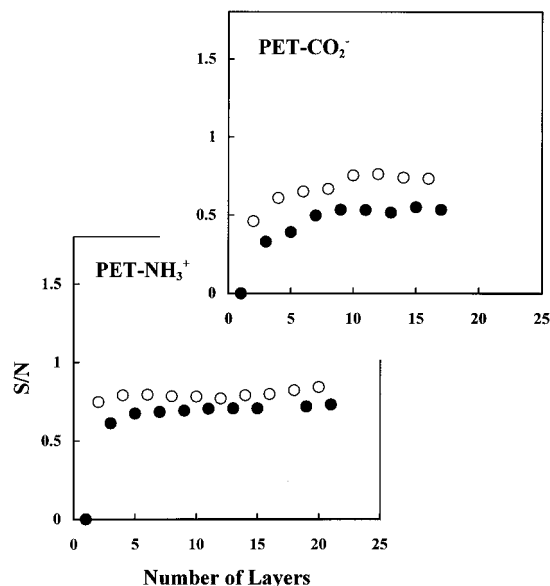


Figure 11. Sulfur:nitrogen atomic ratio data (75° take-off angle) for polyelectrolyte multilayers supported on PET-CO₂⁻ and PET-NH₃⁺ (odd number of layers (●); even number of layers (○)).

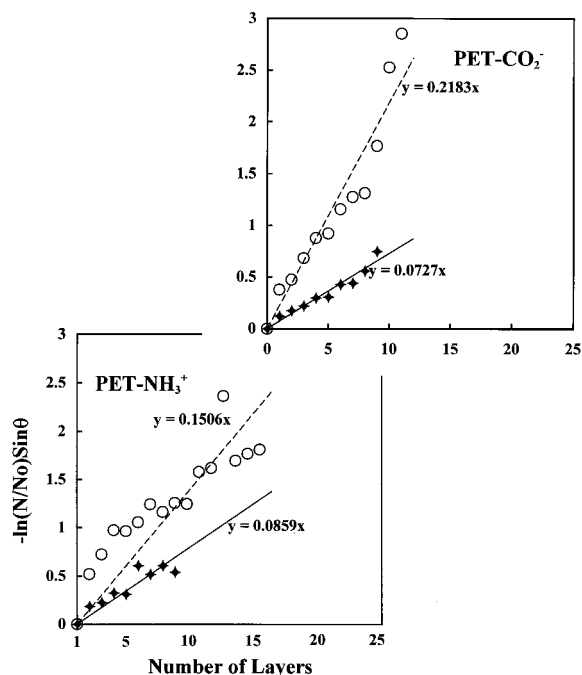


Figure 12. Plots of $-\ln(N/N_0) \sin \theta$ vs number of layers in multilayer films supported on PET-CO₂⁻ and PET-NH₃⁺. The closed (♦) and open (○) symbols are data recorded at 15° and 75° take-off angles, respectively.

(Figure 11). The S:N ratio levels at ~ 0.8 for PET-NH₃⁺ and at ~ 0.65 for PET-CO₂⁻. It is important to note that the initial substrate surface chemistry controls the structure of not just the first, but all of the layers in the multilayer assembly.

Mechanical Properties of Multilayer Assemblies. As discussed in the Introduction, our objective in this work is to develop layer-by-layer deposition as a method to control surface structure and surface properties of solid polymers. For this method to be practical, the multilayer assemblies must have mechanical integrity and must adhere to the substrates. We have carried out simple peel tests using pressure-sensitive adhesive tape to determine the locus of failure in substrate/

multilayer assembly/adhesive tape composites. Peel tests on the three substrates were also performed as control experiments.

The tape was applied and peeled from the samples and XPS spectra of both surfaces were compared with spectra obtained before the adhesive joint was formed. The atomic composition of the tape used (3M no. 810) at 15° take-off angle is C, 87.2%; O, 12.8%. The compositions of PET (C, 71.5%; O, 28.5%) and PET-CO₂⁻ (C, 69.9%; O, 30.1%) are significantly different than that of the tape. The other samples contain nitrogen (PET-NH₃⁺) or both nitrogen and sulfur so the XPS analyses of the locus of failure were straightforward.

The unmodified PET surface composition did not change after the peel test; however, the carbon content of the tape decreased to 84.4%, indicating that cohesive failure in PET occurs. A weak boundary layer, likely consisting of PET oligomers⁵³ transfers from PET to the tape. XPS analysis of an unmodified PET sample supporting 14 layers after the peel test indicated that no nitrogen or sulfur was present. Both nitrogen and sulfur as well as PET oligomers were observed on the tape. This cohesive failure in PET indicates that the multilayer assembly is at least as strong as the weak boundary layer and that there is an adhesive interaction between the first polyelectrolyte layer and PET. The peel tests of PET-NH₃⁺, PET-CO₂⁻, PET-NH₃⁺ with 14 layers, and PET-CO₂⁻ with 10 layers all indicated cohesive failure in the tape. The tape composition remained unchanged and a thin layer of adhesive was apparent in the film spectra. These results indicate that the mechanical strength of the multilayer assemblies and the adhesive strength of the bonds between the multilayers and the charged substrates are stronger than the cohesive strength of the pressure-sensitive adhesive tape.

Summary

Layer-by-layer deposition of polyelectrolytes (PAH and PSS) has been used to build up multilayer films on three organic polymer substrates: PET, PET-CO₂⁻, and PET-NH₃⁺. XPS and contact angle data indicate that the layers are stratified and the wettability of the multilayer assemblies is largely controlled by the identity of the outermost polyelectrolyte layer. The individual layers are extremely thin (2–6 Å), and this thickness is affected by the substrate surface chemistry and can be controlled by adjusting the ionic strength of the polyelectrolyte solutions. The stoichiometry of the deposition process (ammonium ion:sulfonate ion ratio) is also affected by the substrate chemistry and solution ionic strength; it varies significantly in the series of experiments studied, indicating that the layer-by-layer deposition process is quite forgiving and proceeds under a variety of conditions. Peel tests indicate that the multilayer assemblies show good mechanical integrity; no failures were observed in the multilayers. These experiments indicate that layer-by-layer deposition is a viable tool for polymer surface modification.

Acknowledgment. We thank the Office of Naval Research (Contract N00014-92-J-1040) for financial support.

References and Notes

- (1) Decher, G.; Hong, J. D.; Schmitt, J. *Thin Solid Films* **1992**, 210/211, 831.
- (2) Lvov, Y.; Decher, G.; Mohwald, H. *Langmuir* **1993**, 9, 481.

- (3) Keller, S. W.; Kim, H. N.; Mallouk, T. E. *J. Am. Chem. Soc.* **1993**, *115*, 11855.
- (4) Bell, C. M.; Arendt, M. F.; Gomez, L.; Schmehl, R. H.; Mallouk, T. E. *J. Am. Chem. Soc.* **1994**, *116*, 8374.
- (5) Stockton, W. B.; Rubner, M. F. *Polym. Prepr. (Am. Chem. Soc., Div. Polym. Chem.)* **1994**, *35*, 319.
- (6) Cheung, J. H.; Fou, A. C.; Rubner, M. F. *Thin Solid Films* **1994**, *244*, 985.
- (7) Kleinfeld, E. R.; Ferguson, G. S. *Science* **1994**, *265*, 370.
- (8) Mao, G.; Tsao, Y.; Tirrell, M.; Davis, H. T. *Langmuir* **1993**, *9*, 3461.
- (9) Hammond, P. T.; Whitesides, G. M. *Macromolecules* **1995**, *28*, 7569.
- (10) Leväsalmi, J.-M.; McCarthy, T. J. *Polym. Prepr. (Am. Chem. Soc., Div. Polym. Chem.)* **1996**, *37* (1), 457.
- (11) Ferreira, M.; Rubner, M. F. *Macromolecules* **1995**, *28*, 7107.
- (12) Fou, A. C.; Rubner, M. F. *Macromolecules* **1995**, *28*, 7115.
- (13) Swalen, J. D.; Allara, D. L.; Andrade, J. D.; Chandross, E. A.; Garoff, A.; Israelachvili, J.; McCarthy, T. J.; Murray, R.; Pease, R. F.; Rabolt, J. F.; Wynne, K. J.; Yu, H. *Langmuir* **1987**, *3*, 932.
- (14) Dias, A. J.; McCarthy, T. J. *Macromolecules* **1987**, *20*, 2068.
- (15) Lee, K.-W.; McCarthy, T. J. *Macromolecules* **1988**, *21*, 2318.
- (16) Bee, T. G.; McCarthy, T. J. *Macromolecules* **1992**, *25*, 2093.
- (17) Costello, C. A.; McCarthy, T. J. *Macromolecules* **1987**, *20*, 2819.
- (18) Bening, R. C.; McCarthy, T. J. *Macromolecules* **1990**, *23*, 2648.
- (19) Dias, A. J.; McCarthy, T. J. *Macromolecules* **1984**, *17*, 2529.
- (20) Iyengar, D. R.; Brennan, J. V.; McCarthy, T. J. *Macromolecules* **1991**, *24*, 5886.
- (21) Franchina, N. L.; McCarthy, T. J. *Macromolecules* **1991**, *24*, 3045.
- (22) Ward, W.; McCarthy, T. J. In *Encyclopedia of Polymer Science and Engineering*, 2nd ed.; Mark, H. F., Bikales, N. M., Overberger, C. G., Menges, G., Kroschwitz, J. I., Eds.; John Wiley and Sons: New York, 1989; suppl. vol., p 674.
- (23) Werner, E.; Janocha, S.; Hopper, M. J.; Mackenzie, K. J. In *Encyclopedia of Polymer Science and Engineering*, 2nd ed.; Mark, H. F., Bikales, N. M., Overberger, C. G., Menges, G., Kroschwitz, J. I., Eds.; John Wiley and Sons: New York, 1989; Vol. 12, p 193.
- (24) Wang, J.; Feng, D.; Wang, H.; Rembold, M.; Fritz, T. *J. Appl. Polym. Sci.* **1993**, *50*, 585.
- (25) Strobel, M.; Lyons, C. S.; Strobel, J. M.; Kapaun, R. S. *J. Adhes. Sci. Technol.* **1992**, *6*, 429.
- (26) Bertrand, P.; DePuydt, Y.; Beuken, J. M.; Lutgen, P.; Feyder, G. *Nucl. Instrum. Methods Phys. Res., Sect. B* **1987**, *B19-20*, 887.
- (27) Arenolz, E.; Heitz, J.; Wagner, M.; Baeuerle, D.; Hibst, H.; Hagemeyer, A. *Appl. Surf. Sci.* **1993**, *69*, 16.
- (28) Yao, Z. P.; Rånby, B. *J. Appl. Polym. Sci.* **1990**, *41*, 1459.
- (29) Dave, J.; Kumar, R.; Srivastava, H. C. *J. Appl. Polym. Sci.* **1987**, *33*, 455.
- (30) Avny, Y.; Reubenfeld, L. *J. Appl. Polym. Sci.* **1986**, *32*, 4009.
- (31) Bui, L. N.; Thompson, M.; McKeown, N. B.; Romaschin, A. D.; Kalman, P. G. *Analyst* **1993**, *118*, 463.
- (32) Collin, R. J. U. S. Pat. 2,955,954, 1964.
- (33) Desai, N. P.; Hubbell, J. A. *Macromolecules* **1992**, *25*, 226.
- (34) Robinson, R. A. In *CRC Handbook of Chemistry and Physics*, 67th ed.; Weast, R. C., Astle, M. L., Beyer, W. H., Eds.; CRC Press, Inc.: Boca Raton, FL, 1986; D144-D145.
- (35) Arnett, E. M. *Prog. Phys. Org. Chem.* **1963**, *1*, 223.
- (36) Brown, H. C.; McDaniel, D. H.; Hflinger, O. In *Determination of Organic Structures by Physical Methods*, Braude, E. A., Nachod, F. C., Eds.; Academic Press: New York, 1955; p 567.
- (37) The adsorption of PSS to PET was studied as well, but multilayers were not prepared using PSS as a first layer. XPS analysis of a PET sample treated with a PSS solution containing MnCl₂ indicated the following composition: C, 65.86%; O, 33.34%; S, 0.47%; Mn, 0.12%; Na, 0.21%.
- (38) The adsorptions described here are most certainly irreversible.
- (39) A specific enthalpic interaction between PET and the substrate polymer is not necessary for adsorption. The adsorption could be driven by a decrease in interfacial free energy and/or by entropy (release of water molecules from the interface). These factors are discussed in: Shiochet, M. S.; McCarthy, T. J. *Macromolecules* **1991**, *24*, 1441.
- (40) Andrade, J. D. *Surface and Interfacial Aspects of Biomedical Polymers, Surface Chemistry and Physics*; Plenum Press: New York, 1985; Vol. 1, p 176.
- (41) Clark, D. T.; Thomas, H. R.; Shuttleworth, D. *J. Polym. Sci., Polym. Lett. Ed.* **1978**, *16*, 465.
- (42) Clark, D. T.; Thomas, H. R. *J. Polym. Sci., Polym. Chem. Ed.* **1977**, *15*, 2843.
- (43) Hall, S. M.; Andrade, J. D.; Ma, S. M.; King, R. N. *J. Electron Spectrosc.* **1979**, *17*, 181.
- (44) Clark, D. T.; Adams, D. B.; Dilks, A.; Peeling, J.; Thomas, H. R. *J. Electron Spectrosc.* **1976**, *8*, 51.
- (45) Ashley, J. C. *IEEE Trans. Nucl. Sci.* **1980**, *NS-27*, 1454.
- (46) Ashley, J. C.; Williams, M. W. *Radical Res.* **1980**, *81*, 364.
- (47) Ashley, J. C. *J. Electron Spectrosc.* **1982**, *28*, 177.
- (48) Ashley, J. C.; Tung, C. J. *Surf. Interface Anal.* **1982**, *4*, 52.
- (49) Leväsalmi, J.-M. Ph.D. Dissertation: University of Massachusetts, 1996; see data in ref 10 above.
- (50) Reference 40, p 180.
- (51) Odd-even trends in water contact angle data for polyelectrolyte multilayer assemblies have been reported: Yoo, D.; Rubner, M. F. *Antec '95 (Proc. Soc. Plast. Eng.)* **1995**, 2568. Chen, W.; Leväsalmi, J.-M.; Watkins, J. J.; McCarthy, T. J. *Antec '95 (Proc. Soc. Plast. Eng.)* **1995**, 2506.
- (52) The relatively high manganese concentration for the seven-layer sample is anomalous. We have not repeated this experiment.
- (53) Bensnoin, J.-M.; Choi, K. Y. *J. Macromol. Sci., Rev. Macromol. Chem. Phys.* **1989**, *C29*, 55.

MA961096D